Available online at www.sciencedirect.com

ScienceDirect

journal homepage: www.elsevier.com/locate/he

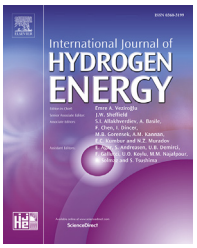

Short Communication

Study on corrosion migrations within catalyst-coated membranes of proton exchange membrane electrolyzer cells

Jingke Mo [a], *Stuart Steen* [a], *Zhenye Kang* [a], *Gaoqiang Yang* [a], *Derrick A. Taylor* [a], *Yifan Li* [a], *Todd J. Toops* [b], *Michael P. Brady* [b], *Scott T. Retterer* [b], *David A. Cullen* [b], *Johney B. Green Jr.* [c], *Feng-Yuan Zhang* [a,*]

[a] *Nanodynamics and High-Efficiency Lab for Propulsion and Power (NanoHELP), Department of Mechanical, Aerospace & Biomedical Engineering, UT Space Institute, University of Tennessee, Knoxville, Tullahoma, TN 37388, USA*

[b] *Oak Ridge National Laboratory, Oak Ridge, TN 37831, USA*

[c] *National Renewable Energy Lab, Golden, CO 80401, USA*

ARTICLE INFO

Article history:
Received 25 June 2017
Received in revised form
7 August 2017
Accepted 1 September 2017
Available online 9 October 2017

Keywords:
Corrosion
Proton exchange membrane
Stainless steel
Migration
Nafion

ABSTRACT

The corrosion of low-cost, easily manufactured metallic components inside the electrochemical environment of proton exchange membrane electrolyzer cells (PEMECs) has a significant effect on their performance and durability. In this study, 316 stainless steel (SS) mesh was used as a model liquid/gas diffusion layer material to investigate the migration of corrosion products in the catalyst-coated membrane of a PEMEC. Iron and nickel cation particles were found distributed throughout the anode catalyst layer, proton exchange membrane, and cathode catalyst layer, as revealed by scanning transmission electron microscopy and energy dispersive X-ray spectroscopy. The results indicate the corrosion products of 316 SS are transported from anode to cathode through the nanochannels of the Nafion membrane, resulting in impeded proton transport and overall PEMEC performance loss.

Introduction

The hydrogen economy is a proposed system of energy storage and delivery which was originally introduced by Dr. J. B. S. Haldane in 1923 [1]. Hydrogen production is a large and growing industry due to its advantages of having a high-energy-density and being environmentally-friendly, and there are still yet many promising applications and uses in the near future [2–7]. The increasing interest in sustainable

* *Corresponding author.*
E-mail address: fzhang@utk.edu (F.-Y. Zhang).

https://doi.org/10.1016/j.ijhydene.2017.09.020

energy systems has driven the development of polymer electrolyte membrane electrolyzer cells (PEMECs) over the past several decades as a hydrogen production method [8–10]. For renewable energy storage and pure hydrogen/oxygen production, PEMECs have several advantages, such as higher energy efficiency/density, faster charging/discharging, and a more compact design [11–13]. The PEMEC decomposes water into separate streams of hydrogen and oxygen by using electrical power. When the energy supply is higher than demand, the excess energy can be stored by producing hydrogen; with the stored hydrogen available for future energy production via, for example a polymer electrolyte membrane fuel cell (PEMFC). This regenerative PEMEC/PEMFC system approach will potentially allow renewable and hybrid energy systems to effectively provide reliable and multi-scale energy by eliminating the intermittence of renewable energy sources [14–16].

Both PEMECs and PEMFCs take advantage of proton exchange membranes (PEM) as electrolytes, which permit the transfer of protons with high efficiency compared to traditional technologies [12,17–20]. Their performance is highly dependent on the properties of the membrane electrode assembly (MEA), and it can be affected by the concentration of various species (proton, water, oxygen, hydrogen, etc.) across and within the cells which can affect the distribution and transport of reactants and products, block active-sites, and lead to overall membrane degradation [21–29].

Liquid/gas diffusion layers (LGDLs) have a central role in the evolution of PEMEC technology. Traditional materials for manufacturing LGDLs are carbon fiber, metals or coated polymers. Metallic LGDLs and bipolar plates have attracted attention in both PEMECs and PEMFCs due to their high bulk electrical conductivity, amenability to rapid manufacturing, and low cost [20,30–41]. However, durability issues remain due to the aggressive electrochemical environment. While carbon paper is widely used as the LGDL in PEMFCs, it is unsuitable in the anode side of PEMECs because it is easily corroded at the high positive potentials and extreme oxidative environments [42]. Metallic LGDLs with higher corrosion resistance are one potential solution. Metal corrosion and ion poisoning on MEAs are critical issues especially for low-cost metals such as stainless steel (SS). It has been reported that metallic cations, especially iron cations, may contaminate the MEA and degrade the performance in PEMFCs. However, to our knowledge, there are few (if any) reports on the electrode corrosion and transport mechanisms/effects in a MEA, especially with metallic LGDLs.

The most popular membrane used in PEMECs and PEMFCs is made of Nafion. Nafion is a sulfonated tetrafluoroethylene-based fluoropolymer-copolymer, which was discovered in the late 1960s by Walther Grot of DuPont [43]. Nafion's unique ionic properties are a result of incorporating perfluorovinyl ether groups terminated with sulfonate groups onto a tetrafluoroethylene (Teflon) backbone [44,45]. Nafion has received a considerable amount of attention as a proton conductor for PEMFCs and PEMECs because of its excellent thermal and mechanical stability.

In our previous work, a 316 SS mesh was intentionally utilized as a model metal anode LGDL to investigate the metal corrosion and transport inside PEMECs during their operations [46]. In this study, further investigations were conducted to gain insight into the behavior of metal cation migration in PEMECs and understand corrosion mechanisms affecting PEMEC performance. The uncoated 316 SS is not a viable candidate for PEMEC LGDLs or bipolar plates due to inadequate corrosion resistance; however, its rapid degradation can be leveraged to study corrosion product migration under PEMEC operating conditions in a reasonable period. Scanning electron microscope (SEM) characterization of both anode and cathode LGDLs before and after testing was performed in our previous study to compare the extent of metal cation migration [46]. In this research, scanning transmission electron microscopy (STEM) and energy-dispersive X-ray spectroscopy (EDS) were used to characterize the incorporation of metal cations introduced into the catalyst-coated membrane (CCM) from SS LGDL corrosion. It was found that migration Fe cation across the CCM resulted in Fe cation accumulation inside the PEM, which severely blocked the transportation of proton from anode to cathode.

Experimental

The CCM investigated in this work came from our previous work of electrochemical investigation of SS corrosion in a PEMEC. The CCM has been operated in the PEMEC for 15 h. All details about the devices, set up, and operation conditions can be found in our previous work [46]. This work builds upon our initial study of the impacts of the corrosion of 316 SS LGDLs on the PEMEC performance, which observed significant Fe cation transport through the membrane, but did not pursue advanced characterization of the membrane. In this study, STEM and EDS are used to characterize the tested CCM to reveal the behavior and mechanism of the Fe cation transfer inside the CCM.

STEM – EDS characterization

A field emission JEOL JSM-6320F SEM with an accelerating voltage of 0.5–30 KV was used for observing the morphological characteristic of the LGDLs before and after testing in a regular PEMEC. A 200 KV JEOL 2200FS FEG – TEM/STEM fitted with a spherical aberration corrector was also used for high-resolution imaging of the IrRuOx and Pt nanoparticle catalyst. It was equipped with a Bruker solid state detector (SDD). Cross-sectional CCM specimens were prepared by diamond knife ultramicrotomy with a target thickness of 50–100 nm.

Results and discussion

The experimental results from our previous work demonstrated that there was severe corrosion at the anode 316 SS LGDL (Fig. 1(a) and (b)), and some of those corrosion products were transported through the CCM, and deposited on the cathode carbon-paper LGDL (Fig. 1(d) and (e)). The SEM images comparing of fresh and operated 316 SS LGDLs at the anode side revealed extensive corrosion of the SS mesh after only 15 h of room temperature operation at a current density of 1.0 A/cm^2 in the PEMEC. Some of corrosion products transported through the CCM and deposited on the surface

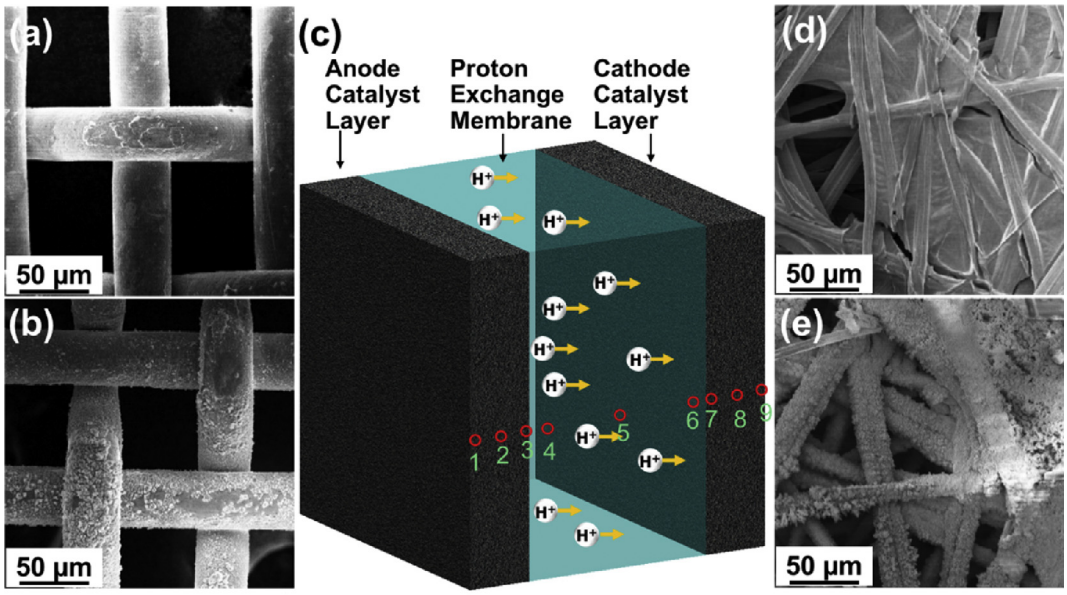

Fig. 1 – SEM image of LGDLs and schematic of proton transporting in CCM. (a) Fresh anode SS LGDL; (b) Tested anode SS LGDL; (c) Schematic of SE-STEM conducted on the tested CCM; (d) Fresh cathode carbon paper LGDL; (e) Tested cathode carbon paper LGDL [46].

of cathode carbon-paper LGDL. Since there were no Fe components at the cathode-side of PEMECs, the deposited Fe cation on the carbon paper must have come from the corrosion of the anode side 316 SS LGDL and transported through the CCM [46].

As shown in Fig. 1(c), the protons are conducted through the PEM from anode to cathode. The mechanism of proton transfer through PEM has been proposed by some scholars [45,47–49]. A recent water channel model was proposed based on simulations of small-angle X-ray scattering data and solid state nuclear magnetic resonance studies [50]. In this model, the sulfonic acid functional groups self-organize into arrays of hydrophilic water channels, each ~2.5 nm in diameter, through which small cations can be easily transported [50]. The efficiency of the proton exchange is highly depended on those hydrophilic water channels. The catalyst layer on both anode and cathode are roughly 15 μm thick. The membrane is made of Nafion 115, whose thickness is around 125 μm.

In this study, ultramicrotome-prepared cross sections of the CCMs were analyzed by STEM-EDS to further investigate the migration behavior of 316 SS corrosion products Fig. 2(a)–(i) show bright-field (BF) and high-angle annular dark-field (HAADF) STEM images of different locations of CCM, which has marked by number in Fig. 1(c). The BF-STEM images of anode catalyst layer are shown in Fig. 2(a)–(c). The dark area in these images is the anode catalyst of IrRuOx, while the white areas represent either the Nafion or the binder epoxy used in the sample preparation process. The HAADF-STEM images of PEM are shown in Fig. 2(d)–(f), the gray background is the Nafion, and the bright regions, like that marked by the red circle, (For interpretation of the references to colour in this figure legend, the reader is referred to the web version of this article.)are Fe oxide particles accumulated and formed clusters in Nafion membrane. The BF-STEM images of cathode catalyst layer are shown in Fig. 2(g)–(i), the dark area is the cathode catalyst of Pt/B. The lighter contrast in Fig. 2(i) is a layer Fe oxide along the back of the cathode.

Higher resolution BF-STEM images of cross sections of both anode and cathode catalyst layers of tested CCM is shown in Fig. 3. As shown in Fig. 3 (a)–(f), the Fe oxide particles are present throughout both catalyst layers, with an average particle size of around 10 nm.

STEM-EDS spectrum images of the CCM cross sections provide additional insight into the migration of the corrosion products. STEM-EDS spectrum images of the IrRuOx anode (Fig. 4(a) and (d)) show Fe cation follows the thicker ionomer layers through the gaps between catalyst IrRuOx. Similar analysis of the membrane (Fig. 4(b) and (e)) show Fe cation dispersed in the whole PEM with some Ni cation. The EDS spectrum images for Fe and Pt (Fig. 4(c) and (f)) show Fe cation coating the carbon-supported Pt catalyst in the cathode.

According to above discovery, the 316 SS LGDL gets corroded at anode side as discussed in our previous research work [46]. Due to the oxygen evolution reaction occurs at the interface between the anode LGDL and CCM, the water at the interface between anode LGDL and catalyst-coated membrane is an acidic environment. The detached ion oxides from LGDLs, which mainly comprise of Fe oxide and Ni oxide, will dissolve in it. Then they uptake and transport in the Nafion along with the water. Since Cr passive are much stronger, Cr oxide barely dissolve into the water. It can be seen that the Fe cation from uncoated 316 SS LGDL permeates the whole CCM, which does not only fill the gaps between anode catalyst of IrRuOx, but also evenly distributes in the Nafion membrane and can be easily found in the gaps between carbon-supported Pt in the cathode. The distribution of Fe cation in the anode, Nafion membrane, and cathode demonstrate that Fe cation readily migrated from the anode to the cathode during the contamination. There was lower content of Nafion in the

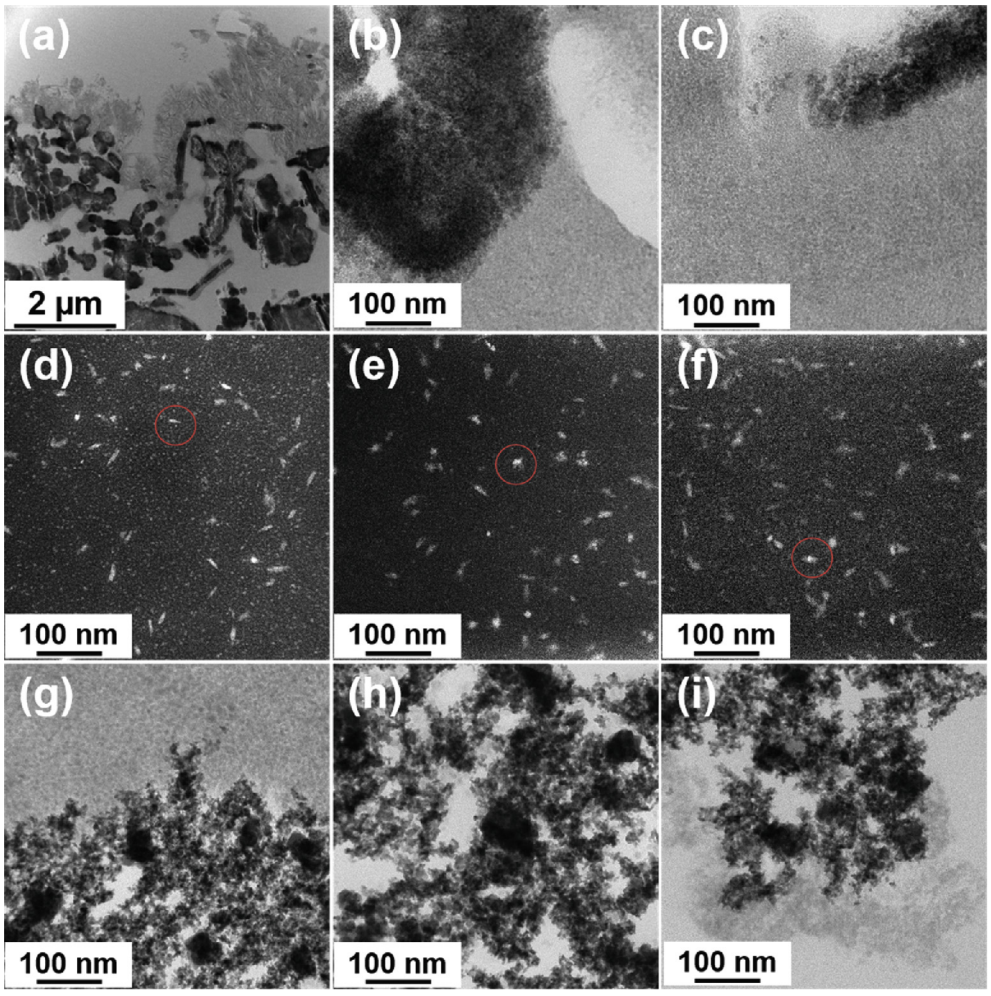

Fig. 2 – BF- and HAADF-STEM images of tested CCM (a)–(f) at different locations marked in Fig. 1 (1)–(9).

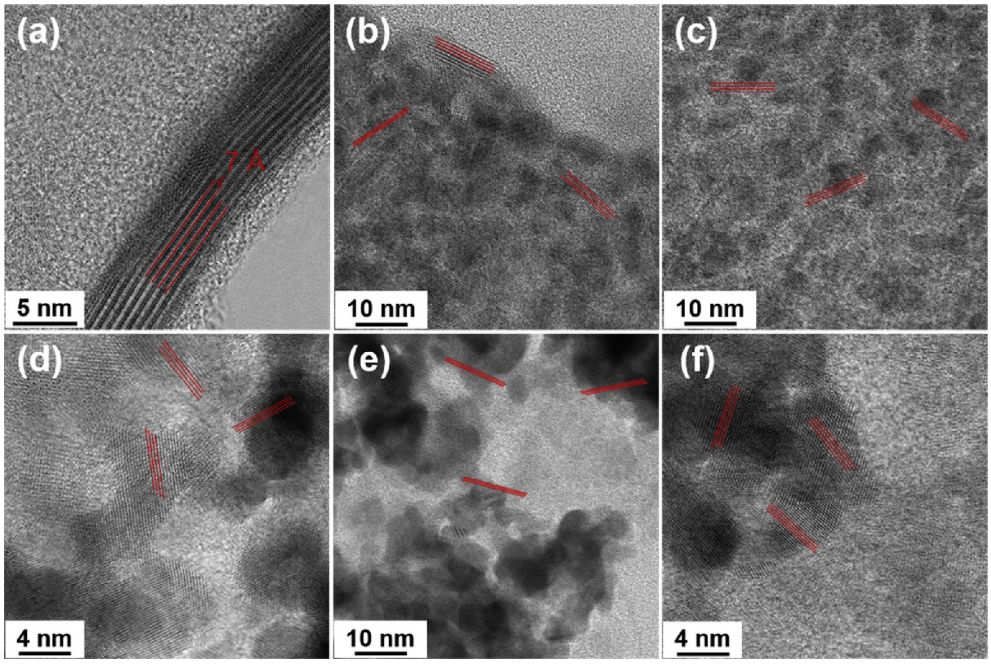

Fig. 3 – BF-STEM images of corrosion products in both anode and cathode catalyst layers at different locations. Images of (a)–(f) are taken from locations of (1)–(3) and (7)–(9) in Fig. 1, respectively.

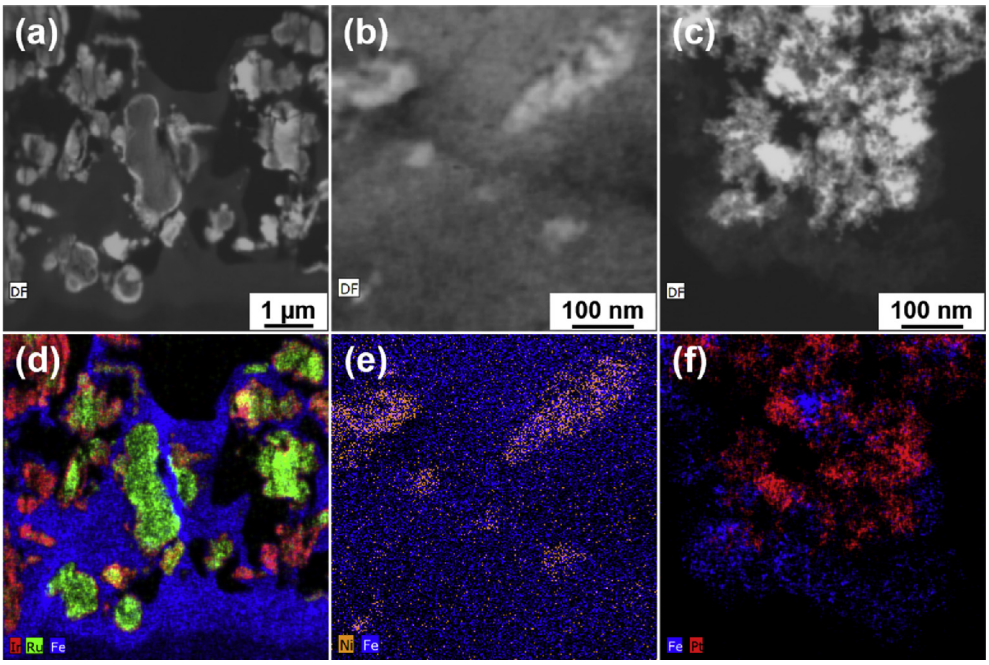

Fig. 4 – HAADF-STEM and EDS spectrum images Fe cation in CCM. (a)–(c) are the HAADF-STEM images of cross section of anode catalyst layer, PEM, and cathode catalyst layer; (d) the EDS spectrum image of Ir, Ru, and Fe in anode catalyst layer; (e) the EDS spectrum image of Ni and Fe in PEM; (f) the EDS spectrum image of Fe and Pt in cathode catalyst layer.

catalyst layers than in the membrane, and Fe cation mainly attached on the sulfonic acid groups in Nafion electrolyte, so the amount of Fe cation in the catalyst layers was smaller than that in the membrane [51–53]. The level of dissolved Fe cations in water have a relationship with local proton concentration. Due to the proton gradient from anode to cathode, some Fe cations might form Fe oxide, stay inside the Nafion membrane and accumulate into Fe oxide clusters or particles with unknown composition as shown in Figs. 2 and 3. Meantime, most of Fe cations attached on the sulfonic acid groups in Nafion electrolyte, transported across the membrane through the water nanochannels [50], and deposited on the cathode carbon paper LGDL, which is observed in Fig. 1(e). Based on the results from our previous and current works, the cation uptake into the MEA from 316 SS follows Fe ≫ Ni ≫ Cr (Cr wasn't found in CCM). A 316 SS LGDL is a good choice to investigate the corrosion migration inside PEMECs due to its low corrosion resistance. It was intentionally selected to investigate metal corrosion product uptake in the MEA during PEMEC operation. Fe cation accumulated in the Nafion membrane, and consequently blocked the water channel for proton transportation, which significantly reduced the efficiency of proton transport from anode to cathode and consequently degrades the PEMEC performance.

Conclusions

Metal cation contamination of Nafion membranes has a significant effect on the performance of devices which use PEM as electrolyte. Building on our previous work, Fe cation is found inside the anode catalyst layer, the proton exchange membrane, and the cathode catalyst layer. A visual demonstration by SE-STEM images shows that, at anode catalyst layer of CCM, high levels of Fe cation fills the gaps between catalyst $IrRuO_x$; Fe cations are also found throughout the membrane and the nickel are also observed in the membrane; at cathode catalyst layer, Fe cation is also found in gaps between the cathode catalyst Pt/B. The uptake into the MEA from 316 SS followings Fe ≫ Ni ≫ Cr (Cr wasn't found in CCM). The EDS images not only identify the exist and distribution of iron and nickel cations inside the CCM, but also tracks the transportation pathways of corrosion from the anode to the cathode inside the CCM. The results indicate the Fe cation mainly attached on the sulfonic acid groups in Nafion electrolyte. The high levels Fe cation exiting in Nafion membrane occupy the water nanochannels in membrane, which would reduce the efficiency of proton transport in PEM and consequently worse the performance of PEMECs, which could be the main reason of corrosion affect the performance of PEMECs. The test and characterization method have been demonstrated to be an effective approach to investigate corrosion migrating across MEAs in both quantitative and qualitative aspects. On the path toward commercialization of PEMECs, contamination and mitigation must be addressed in order to facilitate research and development, which are suggested for future work.

Acknowledgements

The authors greatly appreciate the support from U.S. Department of Energy's National Energy Technology Laboratory

under Award DE-FE0011585. The research was partially performed at ORNL's Center for Nanophase Materials Sciences (CNMS), which is sponsored by DOE Office of Basic Energy Sciences. The authors also wish to express their appreciations to Alexander Terekhov, Douglas Warnberg, and Kate Lansford for their help.

REFERENCES

[1] Haldane JBS. Daedalus or science and the future. New York: EP Dutton; 1924.
[2] Carmo M, Fritz DL, Merge J, Stolten D. A comprehensive review on PEM water electrolysis. Int J Hydrogen Energy 2013;38:4901–34.
[3] Zoulias E, Varkaraki E, Lymberopoulos N, Christodoulou CN, Karagiorgis GN. A review on water electrolysis. TCJST 2004;4:41–71.
[4] Wu H-W. A review of recent development: transport and performance modeling of PEM fuel cells. Appl Energy 2016;165:81–106.
[5] Wang Y, Chen KS, Mishler J, Cho SC, Adroher XC. A review of polymer electrolyte membrane fuel cells: technology, applications, and needs on fundamental research. Appl Energy 2011;88:981–1007.
[6] Peighambardoust SJ, Rowshanzamir S, Amjadi M. Review of the proton exchange membranes for fuel cell applications. Int J Hydrogen Energy 2010;35:9349–84.
[7] Gallucci F, Annaland MVS, Kuipers J. Pure hydrogen production via autothermal reforming of ethanol in a fluidized bed membrane reactor: a simulation study. Int J Hydrogen Energy 2010;35:1659–68.
[8] Wang X, Maeda K, Thomas A, Takanabe K, Xin G, Carlsson JM, et al. A metal-free polymeric photocatalyst for hydrogen production from water under visible light. Nat Mater 2009;8:76–80.
[9] Turner JA. Sustainable hydrogen production. Science 2004;305:972–4.
[10] Medrano J, Spallina V, van Sint Annaland M, Gallucci F. Thermodynamic analysis of a membrane-assisted chemical looping reforming reactor concept for combined H_2 production and CO_2 capture. Int J Hydrogen Energy 2014;39:4725–38.
[11] Grigoriev S, Porembsky V, Fateev V. Pure hydrogen production by PEM electrolysis for hydrogen energy. Int J Hydrogen Energy 2006;31:171–5.
[12] Han B, Steen III SM, Mo J, Zhang FY. Electrochemical performance modeling of a proton exchange membrane electrolyzer cell for hydrogen energy. Int J Hydrogen Energy 2015;40:7006–16.
[13] Kreuter W, Hofmann H. Electrolysis: the important energy transformer in a world of sustainable energy. Int J Hydrogen Energy 1998;23:661–6.
[14] Vanhanen J, Lund P, Tolonen J. Electrolyser-metal hydride-fuel cell system for seasonal energy storage. Int J Hydrogen Energy 1998;23:267–71.
[15] Gasteiger HA, Markovic NM. Just a dream-or future reality? Science 2009;324:48–9.
[16] Lokkiluoto A, Gasik MM. Modeling and experimental assessment of Nafion membrane properties used in SO 2 depolarized water electrolysis for hydrogen production. Int J Hydrogen Energy 2013;38:10–9.
[17] Hoffert MI, Caldeira K, Benford G, Criswell DR, Green C, Herzog H, et al. Advanced technology paths to global climate stability: energy for a greenhouse planet. Science 2002;298:981–7.
[18] Marshall A, Borresen B, Hagen G, Tsypkin M, Tunold R. Hydrogen production by advanced proton exchange membrane (PEM) water electrolysers – reduced energy consumption by improved electrocatalysis. Energy 2007;32:431–6.
[19] Kumbur E, Mench M. Fuel cells–proton-exchange membrane fuel cells| Water Management. 2009.
[20] Ramasamy RP, Kumbur EC, Mench MM, Liu W, Moore D, Murthy M. Investigation of macro-and micro-porous layer interaction in polymer electrolyte fuel cells. Int J Hydrogen Energy 2008;33:3351–67.
[21] Zhang FY, Advani SG, Prasad AK, Beebe TP, Khalifa ZS, Shah SI. Investigation of freeze/thaw effects on catalyst layer degradation in fuel cells with XPS and XRD. Fuel Cell Semin 2009:16–9.
[22] Zhang F-Y, Advani SG, Prasad AK. Advanced high resolution characterization techniques for degradation studies in fuel cells. Polym Electrolyte Fuel Cell Degrad 2011;365.
[23] Chen T, Zhou Y, Liu M, Yuan C, Ye X, Zhan Z, et al. High performance solid oxide electrolysis cell with impregnated electrodes. Electrochem Commun 2015;54:23–7.
[24] Arvay A, French J, Wang JC, Peng XH, Kannan AM. Nature inspired flow field designs for proton exchange membrane fuel cell. Int J Hydrogen Energy 2013;38:3717–26.
[25] Han B, Mo J, Kang Z, Yang G, Barnhill W, Zhang F-Y. Modeling of two-phase transport in proton exchange membrane electrolyzer cells for hydrogen energy. Int J Hydrogen Energy 2017;42:4478–89.
[26] Xu W, Scott K. The effects of ionomer content on PEM water electrolyser membrane electrode assembly performance. Int J Hydrogen Energy 2010;35:12029–37.
[27] Mench MM, Kumbur EC, Veziroglu TN. Polymer electrolyte fuel cell degradation. Academic Press; 2011.
[28] Mališ J, Mazúr P, Paidar M, Bystron T, Bouzek K. Nafion 117 stability under conditions of PEM water electrolysis at elevated temperature and pressure. Int J Hydrogen Energy 2016;41:2177–88.
[29] Jo YY, Cho E, Kim JH, Lim T-H, Oh I-H, Kim S-K, et al. Degradation of polymer electrolyte membrane fuel cells repetitively exposed to reverse current condition under different temperature. J Power Sources 2011;196:9906–15.
[30] Yang G, Mo J, Kang Z, List FA, Green JB, Babu SS, et al. Additive manufactured bipolar plate for high-efficiency hydrogen production in proton exchange membrane electrolyzer cells. Int J Hydrogen Energy 2017;42:14734–40.
[31] Eom K, Cho E, Jang J, Kim H-J, Lim T-H, Hong BK, et al. Optimization of GDLs for high-performance PEMFC employing stainless steel bipolar plates. Int J Hydrogen Energy 2013;38:6249–60.
[32] Wilde PM, Maendle M, Murata M, Berg N. Structural and physical properties of GDL and GDL/BPP combinations and their influence on PEMFC performance. Fuel Cells 2004;4:180–4.
[33] Zhou T, Liu H. Effects of the electrical resistances of the GDL in a PEM fuel cell. J Power Sources 2006;161:444–53.
[34] Mo J, Dehoff RR, Peter WH, Toops TJ, Green JB, Zhang F-Y. Additive manufacturing of liquid/gas diffusion layers for low-cost and high-efficiency hydrogen production. Int J Hydrogen Energy 2016;41:3128–35.
[35] Mo J, Kang Z, Yang G, Retterer ST, Cullen DA, Toops TJ, et al. Thin liquid/gas diffusion layers for high-efficiency hydrogen production from water splitting. Appl Energy 2016;177:817–22.
[36] Mo J, Steen III SM, Han B, Kang Z, Terekhov A, Zhang F-Y, et al. Investigation of titanium felt transport parameters for energy storage and hydrogen/oxygen production. In: 13th international energy conversion engineering conference: AIAA 2015–3914; 2015. p. 3914.

[37] Kang Z, Mo J, Yang G, Retterer ST, Cullen DA, Toops TJ, et al. Investigation of thin/well-tunable liquid/gas diffusion layers exhibiting superior multifunctional performance in low-temperature electrolytic water splitting. Energy & Environ Sci 2017;10:166–75.
[38] Brady MP, Wang H, Yang B, Turner J, Bordignon M, Molins R, et al. Growth of Cr-Nitrides on commercial Ni–Cr and Fe–Cr base alloys to protect PEMFC bipolar plates. Int J Hydrogen Energy 2007;32:3778–88.
[39] Wang H, Brady MP, Teeter G, Turner J. Thermally nitrided stainless steels for polymer electrolyte membrane fuel cell bipolar plates: Part 1: model Ni–50Cr and austenitic 349™ alloys. J Power Sources 2004;138:86–93.
[40] Wang H, Teeter G, Turner J. Investigation of a duplex stainless steel as polymer electrolyte membrane fuel cell bipolar plate material. J Electrochem Soc 2005;152:B99–104.
[41] Taspinar R, Litster S, Kumbur E. A computational study to investigate the effects of the bipolar plate and gas diffusion layer interface in polymer electrolyte fuel cells. Int J Hydrogen Energy 2015;40:7124–34.
[42] Uddin MA, Qi J, Wang X, Pasaogullari U, Bonville L. Distributed cation contamination from cathode to anode direction in polymer electrolyte fuel cells. Int J Hydrogen Energy 2015;40:13099–105.
[43] Del Church S. Firm installs fuel cell. The News Journal. 2006B7.
[44] Heitner-Wirguin C. Recent advances in perfluorinated ionomer membranes: structure, properties and applications. J Membr Sci 1996;120:1–33.
[45] Mauritz KA, Moore RB. State of understanding of nafion. Chem Rev 2004;104:4535–86.
[46] Mo J, Steen SM, Zhang F-Y, Toops TJ, Brady MP, Green JB. Electrochemical investigation of stainless steel corrosion in a proton exchange membrane electrolyzer cell. Int J Hydrogen Energ 2015;40:12506–11.
[47] Simons R. Strong electric field effects on proton transfer between membrane-bound amines and water. Nature 1979;280:824–6.
[48] Freier E, Wolf S, Gerwert K. Proton transfer via a transient linear water-molecule chain in a membrane protein. Proc Natl Acad Sci 2011;108:11435–9.
[49] Luecke H, Richter H-T, Lanyi JK. Proton transfer pathways in bacteriorhodopsin at 2.3 angstrom resolution. Science 1998;280:1934–7.
[50] Schmidt-Rohr K, Chen Q. Parallel cylindrical water nanochannels in Nafion fuel-cell membranes. Nat Mater 2008;7:75–83.
[51] Wang X, Zhang L, Li G, Zhang G, Shao Z-G, Yi B. The influence of Ferric ion contamination on the solid polymer electrolyte water electrolysis performance. Electrochimica Acta 2015;158:253–7.
[52] Goswami A, Acharya A, Pandey A. Study of self-diffusion of monovalent and divalent cations in Nafion-117 ion-exchange membrane. J Phys Chem B 2001;105:9196–201.
[53] Eom K, Cho E, Nam S-W, Lim T-H, Jang JH, Kim H-J, et al. Degradation behavior of a polymer electrolyte membrane fuel cell employing metallic bipolar plates under reverse current condition. Electrochimica Acta 2012;78:324–30.